Journal of Macromolecular Science, Part A
Publication details, including instructions for authors and subscription information:
http://www.informaworld.com/smpp/title~content=t713597274

Phase Behavior of Polymer Blends

Hans-Werner Kammer[a]
[a] Department of Chemistry, Dresden University of Technology, Dresden, German Democratic Republic

To cite this Article Kammer, Hans-Werner(1990) 'Phase Behavior of Polymer Blends', Journal of Macromolecular Science, Part A, 27: 13, 1713 — 1732
To link to this Article: DOI: 10.1080/00222339009351511
URL: http://dx.doi.org/10.1080/00222339009351511

J. MACROMOL. SCI.—CHEM., A27(13 & 14), pp. 1713–1732 (1990)

PHASE BEHAVIOR OF POLYMER BLENDS

HANS-WERNER KAMMER

Department of Chemistry
Dresden University of Technology
Mommsenstrasse 13, DDR-8027 Dresden
German Democratic Republic

ABSTRACT

Major emphasis is placed on the phase behavior of miscible polymer blends. To understand the complex phase behavior of blends, a refined version of an equation-of-state theory is discussed. This theory makes the simultaneous occurrence of upper critical solution temperature and lower critical solution temperature in blends of high molar mass polymers conceivable. The kinetics of isothermal phase dissolution as it emanates from different experimental routes is discussed in terms of Cahn's linearized theory of phase separation. The rate of phase dissolution varies as a function of quench depth, which indicates the rate is directed by both the thermodynamic driving force and the mobility.

1. INTRODUCTION

Polymer blends are combinations of two or even more polymers that can either mix completely on a molecular scale or, as is more often the case, form a two-phase structure. Therefore, with respect to their phase behavior, polymer blends can be characterized as being either miscible or immiscible. The term "miscibility" of polymers will be used for their dispersal at the molecular level.

Miscibility of polymers is expected in three cases:

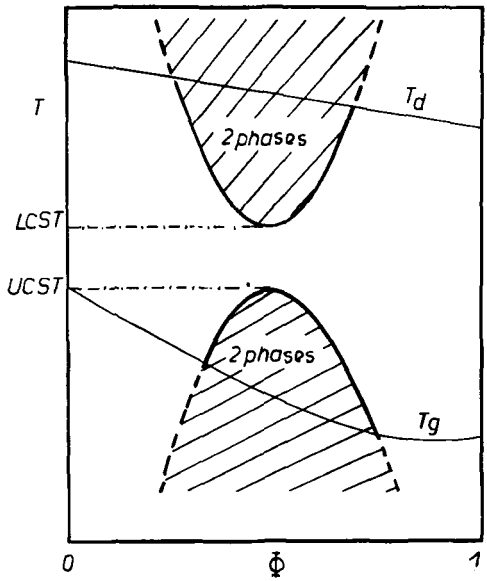

FIG. 1. True equilibrium situations in polymer blends can be observed in the window bounded by the thermal destruction temperature (T_d) and the glass-transition temperature (T_g).

1. Polymers of low molecular mass which have a sufficiently high combinatorial entropy of mixing.
2. Polymers capable of specific interactions leading to favorable (exothermic) heats of mixing [1].
3. A random copolymer turns out to be miscible either with a homopolymer or a second random copolymer when there exists a sufficiently strong "repulsion effect" [2–4].

The phase behavior of polymer blends is experimentally well accessible in a "window" which is bounded at high temperatures by the thermal destruction temperature of the polymeric components, and at low temperatures by the glass transition temperature of the system (cf. Fig. 1). Below the glass transition temperature, the phase behavior can be estimated only tentatively.

Miscible blends, in general, exhibit phase separation at elevated tem-

peratures (Fig. 1). The increase in temperature weakens the specific interactions and the repulsion effect, resulting in a lower critical solution temperature (LCST). Some miscible blends display not only LCST behavior but also phase separation at low temperatures. The decrease in temperature corresponds to a decrease in compressibility. Thus, in turn, it is equivalent to an ascending repulsion between the segments exceeding the specific interactions at an upper critical solution temperature (UCST). The simultaneous occurrence of an LCST as well as an UCST in blends of high molecular weight polymers is considered to be a general phenomenon [5]. However, in most cases the UCST shifts far below the glass transition temperature and, therefore, is not accessible experimentally. When the glass transition temperature is sufficiently low as in systems containing an elastomer as one of the components, the UCST could be confirmed experimentally besides an LCST [6, 7].

Various polymer blends just above the LCST display a very regular, bicontinuous two-phase morphology. This phenomenon conveys the possibility to manipulate and control the phase morphology in polymer blends [8, 9]. It may also be interesting for designing new fibers or membranes based on phase-separated structures. Thus, a largely open field is offered for studies of morphology and structure–property relationships. To exploit thermally induced phase separation for the design of new blend materials, one needs basic knowledge of phase behavior including phase equilibria, dynamics of phase separation, and phase dissolution.

In this paper we mainly discuss phase equilibria and the kinetics of phase dissolution in blends containing random copolymers. Due to their central importance in directing the phase behavior, thermodynamic issues are sketched first. Experimental determination of miscibility areas provides the individual interaction parameters necessary for predictions of various phase equilibria. This is followed by an outline on the phase dissolution kinetics which can be pursued by laser light scattering and will be discussed in terms of Cahn's linearized theory [10].

2. THERMODYNAMICS OF POLYMER–POLYMER MISCIBILITY

According to the Second Law of thermodynamics, the state of miscibility of any mixture is governed by the Gibbs free energy of mixing, ΔG^M. In the framework of a mean-field approximation, ΔG^M of a binary polymer mixture is given by

$$\frac{\Delta G^M}{RT} = \frac{\phi_A}{r_A} \ln \phi_A + \frac{\phi_B}{r_B} \ln \phi_B + X\phi_A\phi_B \tag{1}$$

where r_i and ϕ_i are the degree of polymerization and the volume fraction of component i, respectively. As can be seen, the dimensionless parameter X is a free-energy parameter. According to the thermodynamic theory of polymer mixing, three effects contribute to parameter X [5]:

1. The segmental interaction represented by the parameter X_{AB}.
2. The free-volume effect arising from the different free volumes of the components and represented by the parameter Γ.
3. The size-effect resulting from the differences in the sizes of the segments and represented by the parameter ρ.

As will be shown below, even small values of ρ may have large effects on the sign and value of excess quantities.

The first two terms on the right-hand side of Eq. (1) represent the combinatorial entropy of mixing, $-\Delta S_c^M$. ΔS_c^M is always positive, i.e., a negative contribution to ΔG^M results which corresponds to a stabilization of the mixture. However, in the case of high molecular weights of the components (each r large), ΔS_c^M for polymer blends tends to zero and the entropic stabilization is negligible. This fact suggests that $\Delta G^M < 0$ required for mutual miscibility of polymers can only result when the free-energy parameter X is negative.

The parameter X can be expressed as [5]

$$X = -\frac{U_A}{RT}\left(2X_{AB}^T + \frac{\tilde{V}_A^2}{\tilde{\kappa}_A}\frac{9}{8}\rho^2\right) + \frac{C_{VA}}{2R}\frac{7}{4}\Gamma^2 \tag{2}$$

where

$$X_{AB}^T \equiv X_{AB} + \frac{9}{2}\rho^2 - \frac{3}{8}\rho\Gamma$$

The molar configurational energy $-U_A$, the heat capacity C_{VA}, and the quantity $-U_A\tilde{V}_A^2/\tilde{\kappa}_A$ ($\tilde{\kappa}_A$ being the reduced compressibility) can be replaced by the reduced volume $\tilde{V}_A$ by using a suitable equation of state. After Flory [11], the following equation of state holds between the reduced quantities:

$$\tilde{P} = \frac{\tilde{T}\tilde{V}^{-2/3}}{\tilde{V}^{1/3} - 1} - \frac{1}{\tilde{V}^2} \tag{3}$$

which simplifies in the limit $\tilde{P} = 0$ to

$$\tilde{T} = \frac{\tilde{V}^{1/3} - 1}{\tilde{V}^{4/3}} \tag{3'}$$

$\tilde{V}^{1/3}$ varies in the range 1 . . . 4/3. Employing Eqs. (3) and (3'), one arrives at

$$-\frac{U_A}{RT} = \frac{1}{\tilde{T}_A\tilde{V}_A}, \qquad -\frac{\tilde{V}_A^2 U_A}{\tilde{\kappa}_A RT} = \frac{\tilde{V}_A^{1/3}\left(\frac{4}{3} - \tilde{V}_A^{1/3}\right)}{(\tilde{V}_A^{1/3} - 1)^2},$$

$$\frac{C_{VA}}{R} = \frac{\tilde{V}_A^{1/3}}{\frac{4}{3} - \tilde{V}_A^{1/3}} \tag{4}$$

As can be seen, the quantities $-U_A$, $-U_A\tilde{V}_A^2/\tilde{\kappa}_A$, and C_{VA} are positive definite. Furthermore, the molar configurational energy $-U_A$ and the quantity $-U_A\tilde{V}_A^2/\tilde{\kappa}_A$ are decreasing functions of temperature, whereas the heat capacity C_{VA} ascends with increasing temperature. Equation (2) indicates that the requirement $X < 0$ for miscibility can only be fulfilled when the interaction parameter X_{AB} is negative. For $X_{AB} < 0$, the interaction term of Eq. (2) is also negative and favors mixing. In the case where $\rho = 0$, it dominates the unfavorable free volume term up to a certain temperature. With increasing temperature, the magnitude of the interaction term decreases and the free volume term increases, leading to an increase of the parameter X. At $X = 0$, an LCST occurs followed by phase separation at higher temperatures. As Eqs. (2) and (4) indicate, for $\rho \neq 0$ the second term of Eq. (2) increases with decreasing temperature, resulting again in an ascent of the parameter X. Therefore, the interaction term dominates the unfavorable free-volume and size-effect terms only within a certain range of temperatures, i.e., LCST as well as UCST occurs. The parameter X and its constituents as a function of temperature are depicted in Fig. 2.

Within the limit, the degree of polymerization r tends to infinity when

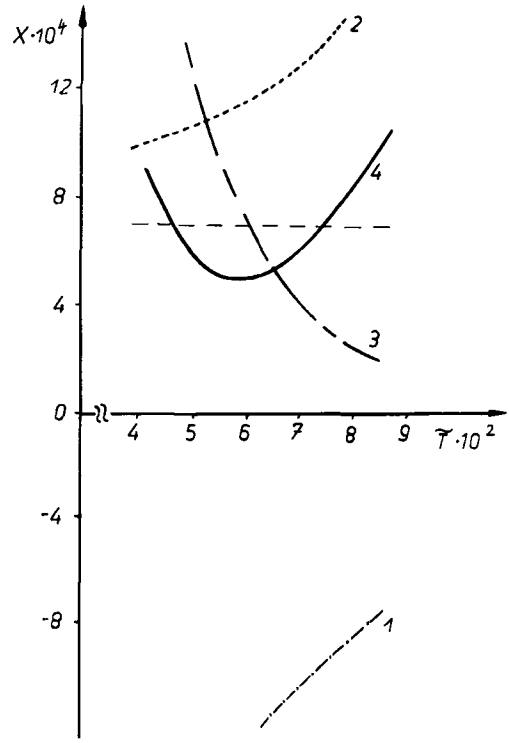

FIG. 2. Variation of the parameter X (Curve 4) and its constituents—interaction (1), free volume (2), and size effect (3)—as a function of reduced temperature according to Eqs. (2) and (4). The parameters used are: $X_{AB}^{T} = -1 \times 10^{-4}$, $\Gamma^2 = 6 \times 10^{-4}$, $\rho^2 = 3 \times 10^{-5}$. The combinatorial entropy of mixing at $\phi = 0.5$ and $r = 1000$ is indicated by the horizontal broken straight line.

UCST and LCST are given by $X = 0$. From Eqs. (2) and (4), it follows approximately:

$$\text{UCST:} \qquad \tilde{V}_A^{1/3} = 1 + \frac{\frac{3}{16}\rho^2}{\frac{9}{16}\rho^2 - X_{AB}^{T}} \tag{5}$$

$$\text{LCST:} \qquad \tilde{V}_A^{1/3} = \frac{4}{3} - \frac{\frac{7}{48}\Gamma^2}{\frac{7}{16}\Gamma^2 - X_{AB}^T} \tag{6}$$

The positions of the UCST and LCST are governed by the parameters ρ and Γ, respectively. This means the UCST is caused by the enthalpic contribution associated with the size effect, whereas the LCST behavior is an entropy-driven process [5].

Another interesting fact results when one calculates the volume of mixing in the same approximation as the Gibbs free energy of Eqs. (1) and (2). It follows:

$$\frac{\Delta\tilde{V}^E}{\tilde{V}_A\phi_A\phi_B} = \frac{3}{4}\rho\left(\Gamma + \frac{11}{9}\rho\right) + \frac{\tilde{V}_A^{1/3} - 1}{\frac{4}{3} - \tilde{V}_A^{1/3}}\left(2X_{AB} + 9\rho^2 + \frac{9}{4}\rho\Gamma\right) + \frac{(\tilde{V}_A^{1/3} - 1)^2}{\tilde{V}_A^{1/3}\left(\frac{14}{9} - \tilde{V}_A^{1/3}\right)}\frac{3}{16}\Gamma^2 \tag{7}$$

When there is no size effect in miscible systems, i.e., $\rho = 0$, and $X_{AB} < 0$, then the volume of mixing ΔV^E is negative. With increasing ρ the sign of ΔV^E will change, whereas ΔG^M keeps the same sign. As a result, $\Delta V^E > 0$ can occur for miscible systems. This effect has been observed in blends of poly(methyl methacrylate) (PMMA) and poly(ethyl acrylate) with poly(vinylidene fluoride) (PVDF) [12]. For the system PMMA/PVDF, the simultaneous occurrence of LCST and UCST has been confirmed (cf. Fig. 3). The LCST and UCST are reported to be about 325 and 140°C for 50/50 blends [13]. These values can be used to estimate the quantities X_{AB} and ρ from Eqs. (5) and (6).

We choose the polymer PMMA as the reference substance A. The thermal expansion coefficients for PMMA and PVDF have been found to be $\alpha = 6.3 \times 10^{-4}\,K^{-1}$ [14] and $7.6 \times 10^{-4}\,K^{-1}$ [15], respectively, in the range of 150 to 200°C. Employing

$$\tilde{V}^{1/3} - 1 = \frac{\alpha T}{3(1 + \alpha T)} \tag{8}$$

and Eq. (3′), one immediately obtains the reference temperatures. It follows that

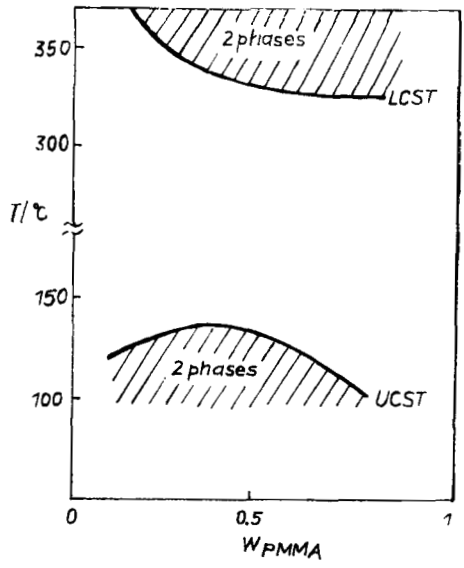

FIG. 3. Phase diagram of PMMA/PVDF, after Ref. 13. LCST behavior was observed in the hatched areas.

$$\text{PMMA: } T_A^* = 8100\ \text{K}; \qquad \text{PVDF: } T_B^* = 7320\ \text{K} \tag{9}$$

The quantity Γ is given by [16]

$$\Gamma = \frac{T_B^*}{T_A^*} - 1 = -0.096; \qquad \Gamma^2 = 9.3 \times 10^{-3} \tag{10}$$

Furthermore, we note after applying Eq. (3'): UCST (at 140°C) and LCST (at 325°C) correspond to $\tilde{V}_A^{1/3} = 1.0658$ and 1.1135, respectively. One can extract from Eqs. (5) and (6) the upper limits of the quantities X_{AB} and ρ. It follows that

$$X_{AB} = -5.2 \times 10^{-3}, \qquad \rho = -0.030, \qquad \rho^2 = 9.2 \times 10^{-4} \tag{11}$$

where X_{AB} agrees pretty well with the result $X_{AB} = -0.007$ submitted in Ref. 17.

Employing the values of the parameters as presented in Eqs. (10) and (11), one can calculate the excess volume according to Eq. (7) for a 50/

50 blend of PMMA and PVDF at 447 K ($\tilde{V}_A^{1/3} = 1.0732$). It is $\Delta V^E/V_A = 1.1 \times 10^{-3}$ again in good agreement with the experimental result 1.9×10^{-3} [12].

In conclusion, the simultaneous occurrence of an LCST and an UCST is associated with positive contributions to the Gibbs free energy of mixing due to the free-volume effect and the differences in segmental sizes, respectively, where the latter effect is most striking at low temperatures. When the size effect is negligible, only LCST behavior is experimentally observable.

3. MISCIBILITY PREDICTIONS

As outlined above, the thermodynamic theory can predict, in principle, the phase behavior of blends. For miscibility on a molecular scale, as a necessary condition, the Gibbs free energy of mixing must be negative. Due to the extremely small value of the combinatorial entropy of mixing in the case of high molecular weight polymers, the only way to get a negative contribution to the Gibbs free energy of mixing [1] is for the overall interaction parameter X_{AB} occurring in Eq. (2) to be negative.

The following discussion will be restricted to blends of poly(styrene-*co*-methyl methacrylate) (SMMA) and poly(styrene-*co*-acrylonitrile) (SAN). It is well known that blends of the homopolymer PMMA and random copolymers of styrene and acrylonitrile are miscible within the range of 9.4 up to 34.4 wt% AN content in the copolymer SAN [18]. In that very range of copolymer composition, the PMMA/SAN blends display miscibility and LCST behavior. The LCST sensitively depends on the copolymer composition. Therefore, for blends containing SAN copolymers of varying AN content, one observes different binodals. This behavior can be rationalized in plots of the phase separation temperature at constant blend composition as a function of copolymer composition. For PMMA/SAN blends, one observes a "window of miscibility" in the temperature–copolymer composition plane as depicted in Fig. 4 [18].

In terms of a mean-field approximation, the overall interaction parameter X_{AB} in a blend containing a homopolymer A (segments of type 1) and a random copolymer B (segments of types 2 and 3) can be expressed as a linear combination of individual segmental interaction parameters χ_{ij} [2–4, 19–21]

$$X_{AB} = \beta\chi_{12} + (1 - \beta)\chi_{13} - \beta(1 - \beta)\chi_{23} \tag{12}$$

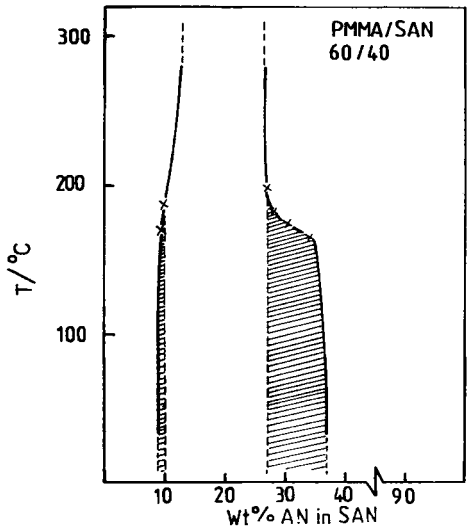

FIG. 4. Miscibility window of PMMA/SAN 60/40 blends [18].

where β represents the mole fraction of component 2 in the random copolymer. As can be seen from Eq. (12), miscibility may occur—at least within a certain range of copolymer composition—if the mutual repulsion between the segments comprising the copolymer exceeds the repulsion between these segments and those in the second component of the mixture.

Employing the theory sketched above, one can extract the individual segmental interaction parameters from the experimentally observed miscibility–immiscibility boundaries as a function of copolymer composition. For blends of PMMA and SAN, it has been found [16] that

$$\chi_{S/MMA} = 0.01, \qquad \chi_{MMA/AN} = 0.05, \qquad \chi_{S/AN} = 0.12 \tag{13}$$

Now, let us turn to blends of two copolymers containing a common segment, i.e., to blends of the type poly(1-*co*-2)/poly(1-*co*-3). Blends of SMMA and SAN are considered as an example for which two limiting cases with respect to the distribution of the components in SMMA copolymers will be discussed: SAN as a random copolymer is blended

with 1) random copolymers of S and MMA units, S-*r*-MMA, and 2) block copolymers containing these components, S-*b*-MMA.

First, we may establish that the same parameters as in Eq. (13) also become operative in blends of the two copolymers SMMA (polymer A) and SAN (polymer B) to regulate the phase behavior. In case 1), the phase behavior is directed by the net interaction parameter X_{AB}, which in analogy to Eq. (12) can be expressed by [4]

$$X_{AB} = x^2\chi_{12} + xy(\chi_{23} - \chi_{13} - \chi_{12}) + y^2\chi_{13} \tag{14}$$

where x and y denote the mole fractions of components 2 and 3 in the respective random copolymers.

As mentioned above, the system PMMA/SAN exhibits a window of miscibility in the temperature–copolymer composition plane. If one gradually replaces MMA units in PMMA by styrene, the range of miscibility with respect to the AN content in SAN must be reduced, finally leading to immiscibility in the limit PS/SAN. In other words, the window of miscibility in S-*r*-MMA/SAN blends shifts with increasing styrene content in S-*r*-MMA to lower AN contents in SAN and, additionally, the range of miscibility shrinks.

A convenient representation of the phase behavior can be made for these systems in the form of an isothermal composition–composition plot displaying the miscibility–immiscibility boundaries as a function of the copolymer compositions. The miscibility domain of SMMA/SAN 50/50 blends at room temperature as estimated by visual inspection of the turbidity of solvent-cast film specimens is shown in Fig. 5. The molecular masses of the S-*r*-MMA and SAN copolymers were all in the order of $M_w = 40{,}000$ and $M_w = 10^5$, respectively.

The curves result from the thermodynamic stability condition and were calculated by using Eqs. (13) and (14). The projection of the miscibility window of PMMA/SAN blends occurs here at the ordinate for AN contents ranging from 9.3 up to 33.8 wt%, in excellent agreement with experimental findings.

From Fig. 5 it may be concluded that the overall agreement between the experimentally determined and theoretically predicted miscibility region is excellent. Therefore, it can be established that knowledge of individual interaction parameters is valuable for the prediction of the phase behavior of blends comprising two random copolymers.

A great deal of interest has also been shown in miscibility of mixtures

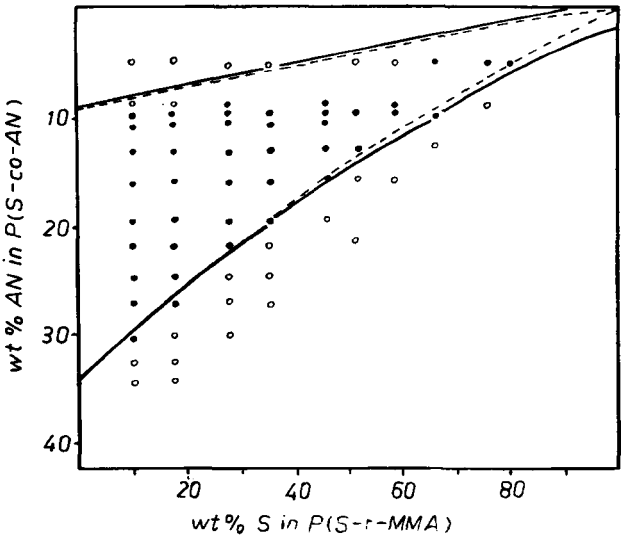

FIG. 5. Miscibility domain for 50/50 blends of S-*r*-MMA and SAN. The experimental data points refer to miscible (●) and immiscible (○) blends. The solid curves were calculated from $\partial^2 \Delta G^M / \partial \phi^2 = 0$ by using Eq. (14), the parameters of Eq. (13), as well as $r_A = r_B = 1000$ and $\vartheta = 160°C$. The broken curves refer to the infinite molecular-mass limit [16].

of block copolymers and the corresponding homopolymers [22–26]. Here, we present results concerning the miscibility of diblock copolymers, S-*b*-MMA, and random copolymers, SAN, as estimated by optical inspection of solvent cast films.

The components again have the same molecular weights as indicated above for the random copolymers. The phase diagram for blends containing S-*b*-MMA and SAN in a 1/1 ratio is shown in Fig. 6 [27]. Within the area bounded by the dashed curves, microphase separation may occur. However, macrophase separation can be observed only outside this domain. For the sake of comparison, the area of miscibility for S-*r*-MMA/SAN blends is indicated by solid curves. The difference in the miscibility behavior of SAN blended with S-*r*-MMA and S-*b*-MMA, respectively, is striking. For a constant content of styrene in the SMMA copolymer, the window of miscibility with respect to the AN content in SAN is remarkably more extended for diblock copolymers than for random copolymers. Obviously, the SAN copolymer dissolves into the

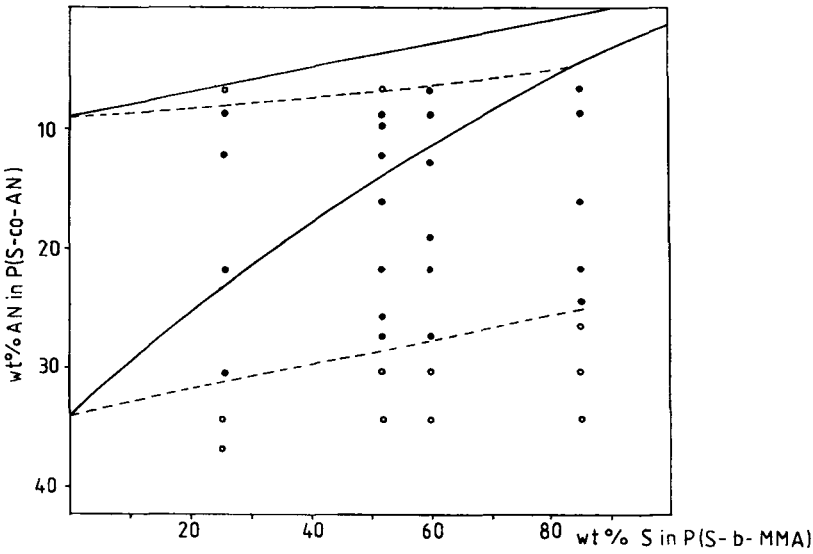

FIG. 6. Miscibility domain for 50/50 blends of S-*b*-MMA and SAN. The broken curves are drawn just to separate the areas of micro- and macrophase separation more clearly. There is no theoretical background behind these curves. The other symbols are as in Fig. 5. The solid curves of Figs. 5 and 6 are identical in meaning.

MMA block of S-*b*-MMA, and this happens at higher AN contents than in mixtures with a random copolymer S-*r*MMA containing the same overall amount of MMA units as the block copolymer. With respect to miscibility, this means that the block copolymer is more similar to the homopolymer, PMMA, than to the random copolymer, S-*r*-MMA. The enthalpic contribution to the Gibbs free energy of mixing resulting from the parameters of Eq. (13) and governing the miscibility of PMMA and SAN seems to prevail over the entropic contributions characteristic for the solubilization of polymers in block domains. It has been shown that this entropic effect is sensitive to the molecular weight ratio of the polymer and the corresponding block of the copolymer [25, 26]. When the ratio exceeds unity, as is the case for the systems under consideration, the entropy change becomes unfavorable for mixing. Here, the sufficiently large negative value of the net interaction parameter exceeds the unfavorable entropic effect within a certain range of the block copoly-

mer composition, and miscibility between the MMA block and SAN occurs. However, the solubility limit is expected to occur if the molecular weights (at high styrene contents) of the MMA block and the SAN become too disparate.

4. KINETICS OF PHASE DISSOLUTION IN POLYMER BLENDS

Many experimental and theoretical studies have been made on the kinetics of phase separation in initially homogeneous polymer mixtures set isothermally into the thermodynamically unstable region [28, 29]. It is the primary objective here to discuss the kinetics of isothermal phase dissolution of phase-separated structures after a rapid temperature jump from the two-phase region into the one-phase region below the lower critical solution temperature. The unmixing in the unstable region proceeds via spinoidal decomposition.

According to Cahn [10], this process is considered to belong to the linear regime, i.e., phase separation is caused by a thermodynamic driving force which initiates a diffusional flux against the concentration gradient. In other words, the unmixing process is treated as being entirely diffusion controlled. This is an approximation which is valid only for small changes in composition. There is experimental evidence that the spinoidal decomposition in the early stage and in the small q regime is described approximately by the Cahn theory [30]. Let R_0 be the size of a polymer coil and q the wavenumber for a particular Fourier component of growing fluctuations. Then the small q domain is characterized by $qR_0 \ll 1$, which means that the wavelength of concentration fluctuations is much larger than the coil diameter. The period of time in which the early stage of spinoidal decomposition is expected to exist can be approximated by $\tau = R^2_0/\tilde{D}$, where $\tilde{D}$ is the apparent diffusion coefficient which governs the rate of phase separation. Thus, the quantity τ describes the time required by a chain molecule to diffuse over a distance comparable to its own size R_0.

The apparent diffusion coefficient is given by [10]

$$\tilde{D} = M \frac{\partial^2_G}{\partial \phi^2} \tag{15}$$

where G is the Gibbs free energy of the mixture in which the concentration of one component is given by a constant value ϕ and M is the mobility constant which is positive.

So far we have discussed the process of phase separation in a thermodynamically unstable region. Analogously, one can study the kinetics of phase dissolution after a rapid temperature jump from the two-phase region into the one-phase region below LCST. Then the phase-separated structures are dissolved by a continuous descent of the thermodynamic driving force responsible for the phase separation. Hence, phase dissolution is the reverse of phase separation, and the theory of phase separation can also be used to discuss the dynamics of phase dissolution. However, unlike the case of phase separation, the linearized theory now describes the late stage of phase dissolution.

In the context of the Cahn theory, it follows for the intensity decay in the diffusion-controlled regime that

$$\ln \frac{I}{I_0} = -2\tilde{D}q^2 t \tag{16}$$

where t is the annealing time after the temperature jump and I_0 is the scattered intensity at annealing time zero. When the scattered intensity decays exponentially, Eq. (16) yields the apparent diffusity $\tilde{D}$ accompanying the dissolution of the two-phase morphology below LCST.

From Eq. (15) it follows that the apparent diffusion coefficient comprises a kinetic aspect, M, as well as a thermodynamic aspect, $\partial^2 G/\partial\phi^2$. If one keeps in mind that the dissolution process progresses after a temperature jump takes place from the two-phase region into the one-phase region, then it is immediately conceivable that M is related to the final state of the temperature jump whereas $\partial^2 G/\partial\phi^2$ characterizes the initial state. Therefore, if one chooses different experimental courses as shown in Fig. 7, one can study the different aspects of $\tilde{D}$. Temperature jumps from one single temperature in the two-phase region to different temperatures in the homogeneous region below LCST (Fig. 7a) correspond to a variation of the mobility M as a function of temperature whereby the thermodynamic driving force is kept constant. The route indicated in Fig. 7(b), on the other hand, focuses attention on the influence of the thermodynamic driving force at constant mobility.

The results are shown in Figs. 8 to 10. The diffusion coefficients governing the phase dissolution below LCST are of the order of 10^{-14} cm^2/s. Figure 8 reflects the influence of the mobility coefficient on phase dissolution. As can be seen, the apparent diffusion coefficient increases with increasing temperature, which solely expresses the temperature dependence of the mobility coefficient. Furthermore, the linear relation-

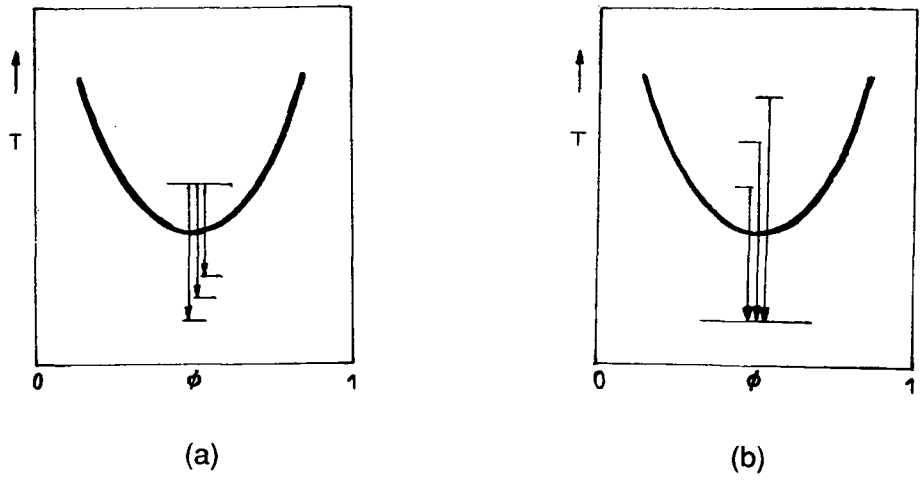

FIG. 7. Courses of the experimental procedure in phase-dissolution experiments. (a) The thermodynamic driving force is kept constant. (b) The mobility remains constant.

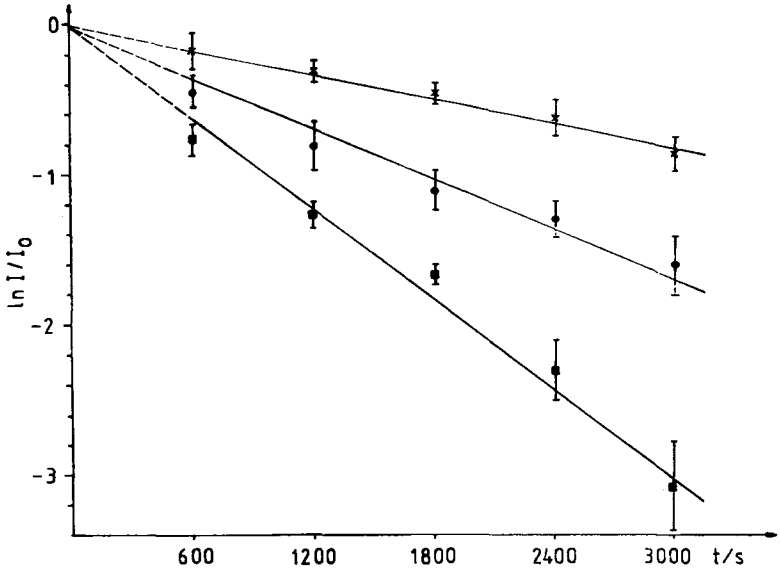

FIG. 8. Changes in the relative scattered intensity after temperature jumps from 210°C to different annealing temperatures below the LCST for the system PMMA/SAN-31.5 (50/50). SAN-31.5 means 31.5 wt% of AN in SAN [31]. (■) 180°C, (●) 160°C, (×) 140°C.

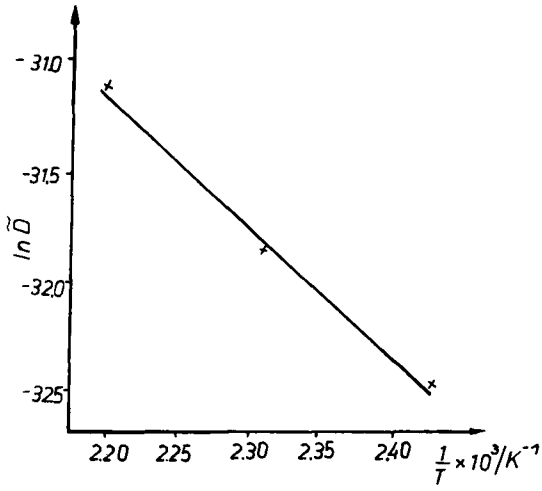

FIG. 9. Arrhenius plot of the apparent diffusion coefficient for the system and the procedure as indicated in Fig. 8 [31].

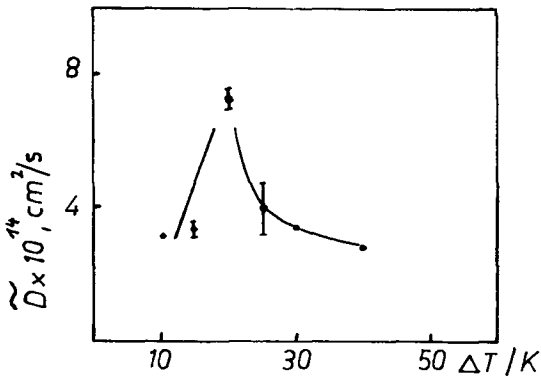

FIG. 10. Apparent diffusity as a function of quench depth for a 50/50 blend of PMMA/SAN-31.5. The phase separation temperature of the blend and the rapid decay of the regular two-phase morphology occur at 200 and 220°C, respectively (cf. text) [34].

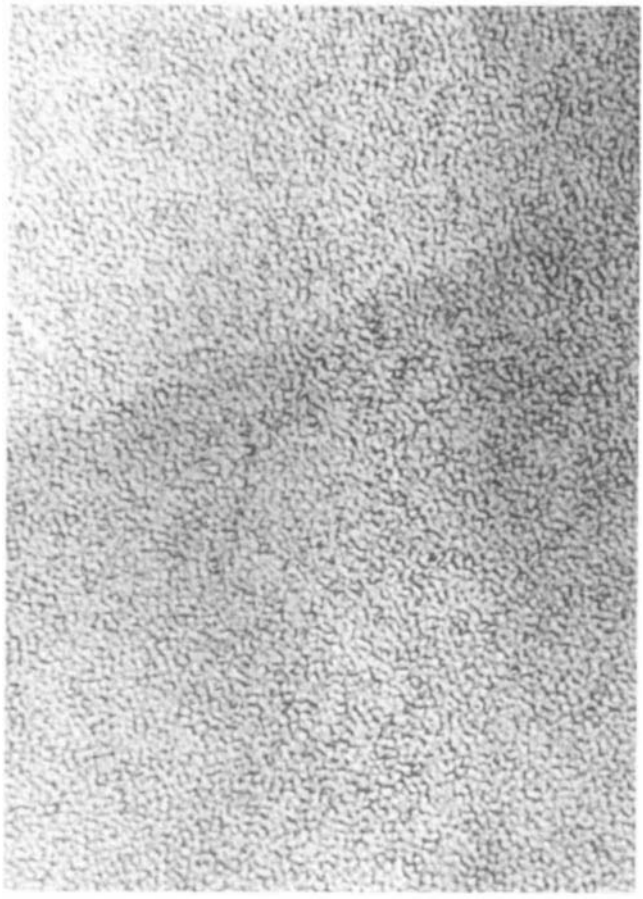

FIG. 11. Light micrograph of the regular two-phase morphology above the binodal; PMMA/SAN-31.5, 60/40 [33].

ship of ln $\tilde{D}$ and $1/T$ suggests that the mobility obeys an Arrhenius-type equation (cf. Fig. 9).

A completely different result occurs if one pursues the experimental course of Fig. 7(b). The variation of the apparent diffusion coefficient as a function of quench depth $\Delta T \equiv T - T_s$, where T_s is the spinoidal point, is presented in Fig. 10. In the first instance, the apparent diffusity increases with increasing quench depth ΔT, which is in accord with the

mean field theory. However, when the quench depth is further raised, the apparent diffusion coefficient starts to decrease.

We have to recognize that various homopolymer/copolymer blends display a very regular, highly interconnected two-phase morphology just above the LCST [32, 33]. An example is shown in Fig. 11. In a certain region of temperature above LCST, this morphology is relatively stable. However, above a certain temperature the regular two-phase structure decays rapidly into an irregular two-phase morphology. The descent of diffusity presumably begins when the temperature approaches the stability limit of the regular two-phase morphology. This result strongly suggests that the thermodynamic driving force depends on the dispersal of the phases in the two-phase region. Hence, the dependence of the thermodynamic driving force on the interfacial energy has to be taken into consideration. If one pays attention to it, at least a qualitative explanation results for the change of the apparent diffusity with quench depth [34].

REFERENCES

[1] D. R. Paul, in *Polymer Blends*, Vol. 1 (D. R. Paul and S. Newman, eds.), Academic, New York, 1978, Chap. 1.
[2] R. P. Kambour, J. T. Bendler, and R. C. Bopp, *Macromolecules, 16*, 753 (1983).
[3] G. ten Brinke and F. E. Karasz, *Ibid., 17*, 815 (1984).
[4] H. W. Kammer, *Acta Polym., 37*, 1 (1986).
[5] H. W. Kammer, T. Inoue, and T. Ougizawa, *Polymer, 30*, 888 (1989).
[6] T. Ougizawa, T. Inoue, and H. W. Kammer, *Macromolecules, 18*, 2089 (1985).
[7] T. Ougizawa and T. Inoue, *Polym. J. (Tokyo), 18*, 521 (1986).
[8] T. Inoue and T. Ougizawa, *J. Macromol. Sci.—Chem., A26*, 147 (1989).
[9] J. Kressler, H. W. Kammer, B. Litauszki, F. Böhme, and M. Rätzsch, *2nd Dresden Polymer Discussion 1989*, Vol. 1, p. 42.
[10] J. W. Cahn, *Acta Metall, 9*, 795 (1961); J. W. Cahn and J. E. Hilliard, *J. Chem. Phys., 28*, 258 (1958).
[11] P. J. Flory, *Disc. Faraday Soc., 49*, 7 (1970).
[12] Y. Li, M. Wold, and J. H. Wendorff, *Polym. Commun., 28*, 265 (1987).

[13] H. Saito, Y. Fujita, and T. Inoue, *Polym. J. (Tokyo), 19*, 405 (1987).
[14] J. Brandrup and E. H. Immergut, *Polymer Handbook*, Wiley-Interscience, New York, 1966.
[15] G. ten Brinke, A. Eshuis, E. Roerdink, and G. Challa, *Macromolecules, 14*, 867 (1981).
[16] H. W. Kammer, J. Kressler, B. Kressler, D. Scheller, H. Kroschwitz, and G. Schmidt-Naake, *Acta Polym., 40*, 75 (1989).
[17] B. Reidl and R. E. Prud'homme, *J. Polym. Sci., Polym. Phys. Ed., 26*, 1769 (1988).
[18] M. Suess, J. Kressler, and H. W. Kammer, *Polymer, 28*, 957 (1987).
[19] G. ten Brinke, F. E. Karasz, and W. J. McKnight, *Macromolecules, 16*, 1827 (1983).
[20] D. R. Paul and J. W. Barlow, *Polymer, 25*, 487 (1984).
[21] F. E. Karasz, *Adv. Chem. Ser., 211*, 67 (1986).
[22] D. J. Meier, *Polym. Prepr., 18*, 340 (1977).
[23] R. J. Roe and D. Rigby, *Adv. Polym. Sci., 82*, 103 (1987).
[24] M. Jiang, X. Huang, and T. Yu, *Polymer, 24*, 1259 (1983); *26*, 1689 (1985).
[25] H. Xie, Y. Liu, M. Jiang, and T. Yu, *Ibid., 27*, 1928 (1986); *Makromol. Chem., Rapid Commun., 9*, 79 (1988).
[26] E. Helfand, *Macromolecules, 8*, 552 (1975); *J. Chem. Phys., 62*, 999 (1975).
[27] J. Kressler, F. E. Karasz, H. W. Kammer, U. Morgenstern, *Makromol. Chem., 191*, 1623 (1990).
[28] T. Nose, *Phase Transitions, 8*, 245 (1987).
[29] T. Hashimoto, in *Dynamics of Ordering Processes* (S. Komura and H. Furukawa, eds.), Plenum, New York, 1988, p. 421; in *Current Topics in Polymer Science* (R. M. Ottenbrite, L. A. Utracki, and S. Inoue, eds.), Hauser, New York, 1987, p. 199.
[30] T. Izumitani and T. Hashimoto, *J. Chem. Phys., 83*, 3694 (1985).
[31] J. Pigłowski, J. Kressler, and H. W. Kammer, *Polym. Bull., 16*, 493 (1986).
[32] T. Nishi, *J. Macromol. Sci.—Phys., B17*, 517 (1980).
[33] J. Kressler, H. W. Kammer, and K. Klostermann, *Polym. Bull., 15*, 113 (1986).
[34] J. Pigłowski, H. W. Kammer, and J. Kressler, *Polymer, 30*, 1705 (1989).